Talanta 164 (2017) 121–127

Contents lists available at ScienceDirect

Talanta

journal homepage: www.elsevier.com/locate/talanta

A multi-walled carbon nanotubes based molecularly imprinted polymers electrochemical sensor for the sensitive determination of HIV-p24

Ya Ma, Xiao-Lei Shen, Qiang Zeng, Hai-Shui Wang, Li-Shi Wang*

School of Chemistry and Chemical Engineering, South China University of Technology, Guangzhou 510641, People's Republic of China

ARTICLE INFO

Keywords:
Human immunodeficiency virus p24
Multi-walled carbon nanotubes
Molecularly imprinted polymers
Electrochemical sensor
Modified electrode

ABSTRACT

To develop a rapid, simple and sensitive method for the determination of human immunodeficiency virus p24 (HIV-p24), a novel molecularly imprinted polymers (MIPs) electrochemical sensor was constructed on the surface of a multi-walled carbon nanotubes (MWCNTs) modified glassy carbon electrode (GCE) by surface polymerization using acrylamide (AAM) as functional monomer, N,N′-methylenebisacrylamide (MBA) as cross-linking agent and ammonium persulphate (APS) as initiator. Each modification step was carefully examined by cyclic voltammetry (CV), differential pulse voltammetry (DPV) and scanning electron microscope (SEM). The proposed MIPs electrochemical biosensor exhibited specific recognition to HIV-p24 and displayed a broad linear detection range from 1.0×10^{-4} to 2 ng cm^{-3} with a low detection limit of 0.083 pg cm^{-3} (S/N=3). This performance is superior to most HIV-p24 sensors based on other methods. Meanwhile, this sensor possessed of good selectivity, repeatability, reproducibility, stability and was successfully applied for the determination of HIV-p24 in real human serum samples, giving satisfactory results. The accuracy and reliability of the sensor is further confirmed by enzyme-linked immunosorbent assay (ELISA).

1. Introduction

Acquired immune deficiency syndrome (AIDS), a severe communicable immune deficiency disease caused by a retrovirus-the human immune deficiency virus (HIV), considered as a serious pandemic and actively spread all over the world. Up to now, there are still no efficacious therapeutic measures, and the analysis laboratory diagnosis of HIV infection is a crucial aspect of controlling AIDS [1,2]. HIV-1 is found in most HIV strains in the eastern and western countries, it can mirrors the replication of the virus in lymphoid tissue. Therefore, the early diagnosis and monitoring of HIV-1 infection in HIV patients are the most important for the control and the antiviral therapies AIDS. HIV-p24 antigen is the HIV-1 capsid protein, appears at an earlier stage of HIV infection than its antibodies, so the early diagnosis of HIV-p24 antigen would be of greater value in preventing and controlling AIDS [1]. Various techniques and strategies have been developed for the determination of HIV-p24, such as fluoroimmunoassay [3,4], radioimmunoassay [5,6], and enzyme-linked immunosorbent assay (ELISA) [7,8], and so on. Some of them have enabled high-throughput detection and have been successfully applied in clinical diagnosis [9]. However, most of these methods have suffered many drawbacks in their applications, such as low sensitivity, complicated operating procedures, and long analysis times, and these would limit the rapid determination of HIV-p24. Therefore, it would be highly desirable to develop a rapid and highly sensitive method to directly identify HIV-p24 antigens.

Molecular imprinting technique, which allows the formation of specific recognition sites in synthetic polymers through the use of template molecules, has become a well-established analytical tool for molecular recognition. These specific receptor sites have high selective recognition to the template molecules over its structurally related compounds. Thus, molecularly imprinted polymers (MIPs) can be used in applications which relying on specific molecular binding events [10–13]. This feature together with its other obvious advantages such as chemical and thermal stability, physical robustness, simplicity and low cost in preparation, make MIPs widely applied in sensing applications, in particular, become a promising method for biomolecules recognition [14]. Electrochemical assays is a promising approach with advantages such as low cost, low power requirements, easy signal quantification, rapidness, and high repeatability, which have attracted considerable interest in recent years [15]. So far, several studies have been published with respect to the preparation of MIPs based electrochemical sensors for the determination of various substances, including oxytetracycline [15], dopamine [16], 3-indoleacetic acid [17], quinoxaline-2-carboxylic acid [18] and proteins, like Myo [19] and Hb [20].

MIPs are usually synthesized by the copolymerization of functional

* Corresponding author.
E-mail address: wanglsh@scut.edu.cn (L.-S. Wang).

http://dx.doi.org/10.1016/j.talanta.2016.11.043
Received 30 August 2016; Received in revised form 19 November 2016; Accepted 20 November 2016
Available online 21 November 2016

monomers and cross-linker in the presence of a template, and the special tailor-made binding sites can be obtained after the remove of template molecules [21]. Although this method is simple and effective, the obvious shortcomings like low rate of mass and electronic transfer and low sensitivity have greatly limited its practical applications [22]. In order to overcome these shortcomings and meet the increasing demands of template for ultrasensitive detection of template at the early stage, great efforts have been devoted to enlarge the current signal to get more sensitive response [23,24]. Based on this fact, nano materials, especially multi-walled carbon nanotubes (MWCNTs) have been widely utilized as an ideal supporting material on account of their unique structures, high stabilities, low resistivities, and high surface-to-volume ratios. For example, Qian et al. reported the in situ chemical oxidative polymerization of pyrrole on MWCNTs surface for the preparation of novel MWCNTs@MIP [16]. Kan et al. reported the immobilization of vinyl group on the surface of MWCNTs for the selective determination of dopamine [25]. Chitosan is a natural cationic biopolymer, with advantages like excellent film-forming ability, high mechanical strength and adhesion and biocompatibility, which had been used to modify electrodes [26]. The MWCNTs/CS composites with rich branched amine groups have been reported to possess massive interesting structural and functional properties and can be expected to be an important intermediate material for various applications [27]. However, to the best of our knowledge, few reports have employed the composites of multi-walled carbon nanotubes/Chitosan (MWCNTs/CS) as reinforcement materials to prepare MIPs. CS not only used as a fundamental to adsorb glutaraldehyde (GA) and further to immobilize HIV-p24 but also plays a key role for the enhancement of sensitivity and stability due to its advantages above [28,29].

The aim of this study is to fabricate an electrochemical sensor based on MIPs for the highly sensitive and selective determination of HIV-p24. To achieve this object, a bare GCE was firstly modified with MWCNTs to enhance the electrical conductivity and increase the specific surface area, and then assembled with CS and a layer of GA for HIV-p24 attachment, following through an polymerization to form a polymer film, finally eluting the template to get MIPs. Each step of the fabrication has been fully characterized by CV and DPV. The prepared MIPs/MWCNTs/GCE exhibits admirable sensitivity and selectivity and successfully applied to the detection of HIV-p24 in real samples.

2. Materials and methods

2.1. Chemicals

Human immunodeficiency virus p24 (HIV-p24), Carcino embryonie antigen (CEA), Human chorionic gonadotropin (HCG), Alpha fetal protein (AFP), Bovine serum albumin (BSA) and HIV-p24 ELISA kit were purchased from Linc-Bio Science Co. Ltd (Shanghai, China). Multi-walled carbon nanotubes (MWCNTs) from Nanoport. Co. Ltd. (Shenzhen, China) were treated with nitric acid and sulfuric acid to get the COOH groups before use. Chitosan (CS, 99% deacetylation) and glutaraldehyde (GA, 25% aqueous solution) were obtained from Sigma-Aldrich Chemical Co. (St. Louis, MO, USA). N,N-methylenebisacrylamide (MBA, Fluka), acrylamide (AAM, Fisher Bioreagents), ammonium persulphate (APS), acetic acid and methanol were purchased from J & $2K Scientific Ltd. (Beijing, China). Tris-HCl buffered solution (20 mM, pH8.0) was prepared by dissolving the Trisbase into water and then adjusted pH by adding suitable volumes of concentrated hydrochloric acid freshly prepared. 0.1 M PBS was prepared by mixing the stock solutions of KH_2PO_4 and K_2HPO_4 and used as working solution. All chemicals were of analytical reagent grade. All the water used in experiments was the hyperpure water (resistivity=18.2 M Ω cm).

2.2. Apparatus

Electrochemical measurements of cyclic voltammetry (CV) and differential pulse voltammetry (DPV) were performed on a CHI 660B electrochemical workstation (Chenhua, Shanghai, China), where a three-electrode configuration was employed consisting of a bare or modified GCE working electrode, a platinum wire auxiliary electrode, and a saturated calomel reference electrode (SCE). CV measurements were carried out in 10 ml of 10 mmol dm^{-3} $K_3[Fe(CN)_6]/K_4[Fe(CN)_6]$ aqueous solution containing 0.1 mol dm^{-3} KCl between −0.2 V and 0.6 V at a scan rate of 50 mV s^{-1}. In DPV measurements, the scan was performed from −0.2–0.6 V at a scan rate of 50 mV s^{-1}. All of the potentials were with respect to SCE. The scanning electron micrographs were taken with field emission scanning electron microscopy (FE-SEM; Zeiss Ultra55, Germany).

2.3. Preparation of the imprinted and non-imprinted film modified electrodes

Prior to the fabrication, a bare glassy carbon electrode (GCE) (3 mm diameter) was polished with 0.3 and 0.05 μm alumina powder, followed by washing with absolute alcohol and hyperpure water between each polishing step in ultrasonic bath for 5 min.

The HIV-p24-imprinted film modified electrodes were prepared as following steps shown in Fig. 1: (i) The prepared MWCNTs were dispersed in deionized water by ultrasonication for 1 h to get a homogenous suspension (0.5 mg dm^{-3}). 5 μL of the treated MWCNTs was deposited on electrode and dried under infrared lamp for 15 min. (ii) After the drying, 1 μL of 0.05 mg dm^{-3} CS was coated on the as-prepared electrode and dried at room temperature, which made the formation of an amine layer on the electrode surface. (iii) The resulted electrode was activated with 2.5% GA (in 50 mM, pH 7.4 phosphate buffer) for 2 h and washed with water to make the aldehyde groups connected to the electrode surface. (iv) 5 μL of 50 μg cm^{-3} HIV-p24 was then applied to the working electrode, reacted at room temperature for 1 h and then put into a 4 ℃ refrigerator for 12 h. Through this process, HIV-p24 protein were covalently linked to the electrode surface through imine bond formed between amino of the protein and aldehyde groups of glutaraldehyde. (v) Immerse the electrode in a 2 ml solution containing 0.213 g AAM as the functional monomer and 0.0324 g MBA as the cross-linker for a while. After that, 0.0411 g (1 ml, 0.06 mol dm^{-3}) APS solution was added to trigger the polymerization. This polymerization was carried out at room temperature for 5 h with N_2, then the sensor was thoroughly washed with hyperpure water. (vi) The sensor was incubated in a 10% (v/v) acetic acid solution containing 10% (w/v) sodium dodecylsulfate (SDS) for 2 h to remove the template [30]. Acetic acid is able to break hydrogen bonds, allowing a successful elution of the protein from the imprinted layer and release the

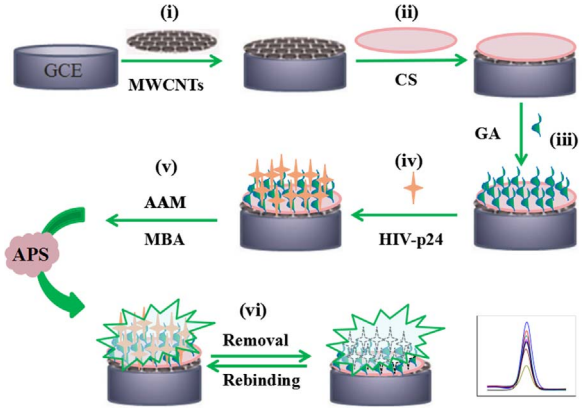

Fig. 1. Detailed procedure diagram for fabrication of the HIV-p24-MIPs/MWCNTs/GCE sensor.

aldehyde group. The electrodes were washed with Tris-HCl buffer again to remove the HIV-p24 produced by acetic acid solution containing 10% (w/v) sodium dodecylsulfate (SDS) treatment. MIPs were successfully prepared on the surface of electrode (MIPs/MWCNTs/GCE).

A non-MIPs modified electrode (NIPs/MWCNTs/GCE) was also prepared with the similar procedure in the absence of the HIV-p24 template.

3. Results and discussion

3.1. Morphological Characterization of MIPs/MWCNTs/GCE

All samples were sputtered with a thin layer of gold before imaging. The SEM images of the glassy carbon electrode before and after modification with MWCNTs were shown in Fig. 2A and Fig. 2B. As observed, MWCNTs are well dispersed on the modified electrode surface. Compared with Fig. 2B, it is obviously noticed in Fig. 2C that a layer of chitosan film was decorated on the surface of MWCNTs through its well film-forming ability. The morphologies of polymer electrode with and without HIV-p24 were shown in Figs. 2D and E, respectively. It can be seen that after the polymerization reaction, the nanotubes structure turned to be highly cross-linked and exhibit a rough surface, indicating the formation of polymer membranes over the surface of GCE (Fig. 2D). After the removal of the template molecules, the electrode surface becomes much rougher (Fig. 2E) due to the formation of imprinted cavities.

3.2. Electrochemical characterization

To confirm the formation of the MIPs/MWCNTs/GCE sensor, CV and DPV responses of a bare electrode and modified electrodes are compared and shown in Fig. 3. It can be seen from Fig. 3A that there are great differences in the cyclic voltammetry curves of the bare GCE (a), MWCNTs/GCE (b), CS/MWCNTs/GCE (c), GA/CS/MWCNTs/GCE (d), HIV-p24/GA/CS/MWCNTs/GCE (e), respectively. As expected, a characteristic reversible redox process of $[Fe(CN)_6]^{3-/4-}$ was observed at the bare GCE electrode (Fig. 3A, curve a). When the electrode was modified with MWCNTs, an obvious increase of the redox peak current was obtained (Fig. 3A, curve b), This is attributed to the good electrical conductivity and high surface-to-volume ratio of the MWCNTs. Subsequently, when modifying the MWCNTs/GCE electrode with CS, the redox peak currents also had some improvement (Fig. 3A, curve c). The reason for this observation was that the CS not only provided the amino but also played an important role in providing the

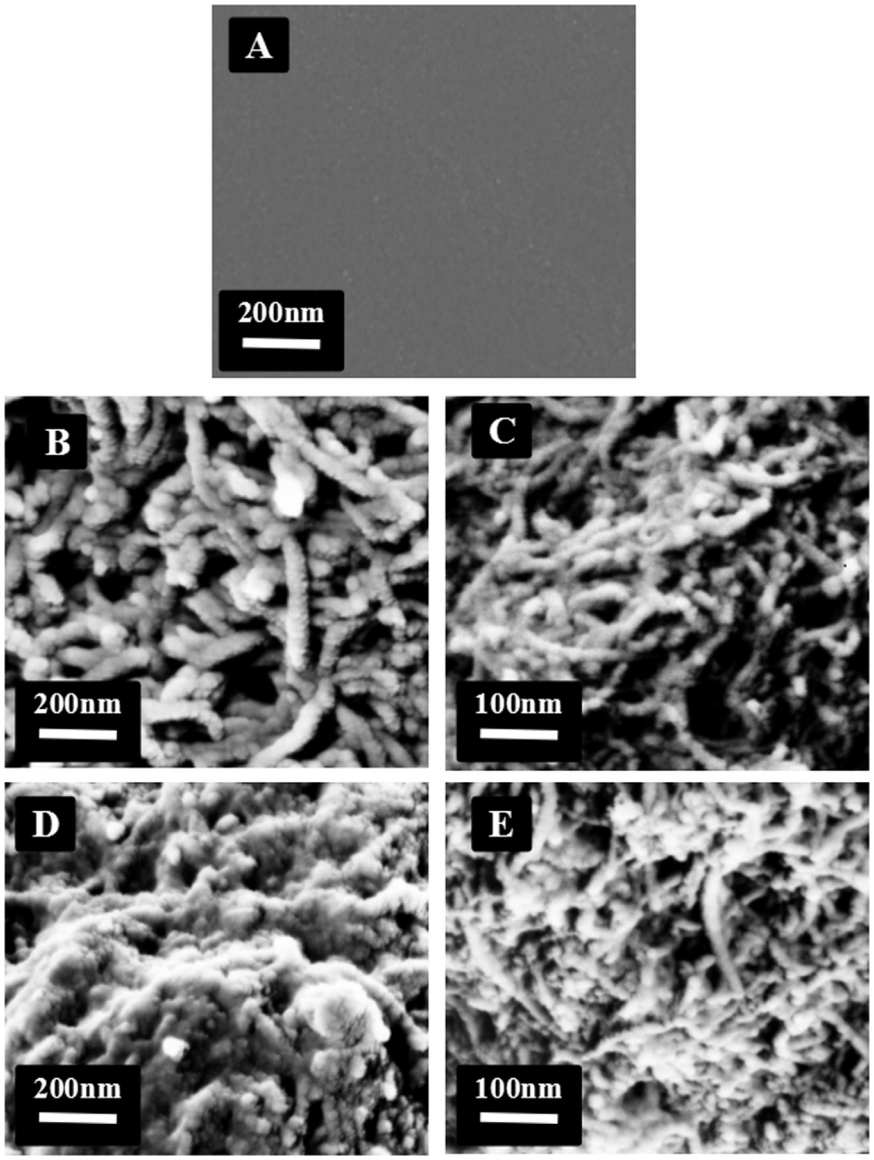

Fig. 2. SEM photographs of the bare GCE (A), MWCNTs /GCE (B), CS/MWCNTs/GCE (C), MIPs/MWCNTs/GCE with template (D), MIPs/MWCNTs/GCE (E).

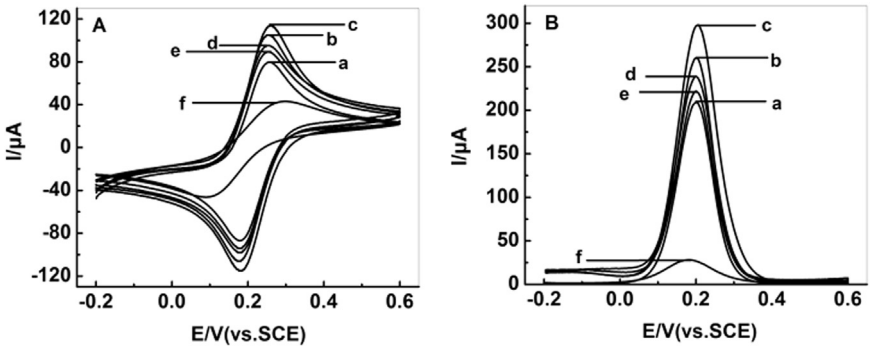

Fig. 3. The CV (A) and DPV (B) characterization of the stepwise modified electrodes (a-bare GCE; b-MWCNTs/GCE; c-CS/MWCNTs//GCE; ɒd-GA/CS/MWCNTs/GCE; e-HIV-p24/GA/CS/MWCNTs/GCE; f-HIV-p24/GA/CS/GCE) in PBS (pH 7.0) containing 10 mmol dm^{-3} $[Fe(CN)_6]^{3-/4-}$ and 0.1 mol dm^{-3} KCl.

conducting bridges for the electron-transfer of $[Fe(CN)_6]^{3-/4-}$. After HIV-p24 were assembled to the amino-CS/MWCNTs/GCE modified electrode by the GA through the -CHO of GA and the $-NH_2$ of HIV-p24 (curve d), the current decreased greatly (curve e), which indicates that HIV-p24 has been successfully immobilized on the electrode surface, by acting as an electron communication and mass-transfer blocking layer to insulate the electron transfer between ferricyanide and the electrode. Meanwhile, the same trend of the current change of $[Fe(CN)_6]^{3-/4-}$ was observed on the electrode at different stages of modification by DPV (Fig. 3B). It also confirmed the successful modification of the GCE. Moreover, the current responses obtained from the HIV-p24/GA/CS modified electrode but without the involvement of MWCNTs are significantly weak (curve f in Figs. 3A and B) compared with HIV-p24/GA/CS/MWCNTs modified GCE (curve e in Figs. 3A and B), indicating the superior electrocatalytical property of MWCNTs.

The electrochemical behaviors of both MIPs/MWCNTs/GCE and NIPs/MWCNTs/GCE investigated by DPV due to its higher sensitivity compared with CV were shown in Figs. 4A and B. The peak current of the MIPs/MWCNTs/GCE electrode after the removal of HIV-p24 (Fig. 4A, curve b) was greatly higher than that of the electrode before the removal (Fig. 4A, curve a). This result points out the imprinted cavities produced in the imprinted membranes after the removal of template can enhance the diffusion of $[Fe(CN)_6]^{3-/4-}$ and promote the redox reaction of $[Fe(CN)_6]^{3-/4-}$ ion pair on the sensor surface. When the electrode was incubated in 0.01 ng cm^{-3} HIV-p24 for 10 min [17], the peak current decreased evidently (Fig. 4A, curve c), indicating the rebound HIV-p24 blocked the penetrating of the probe. In addition, the peak current of curve b was still larger than that of curve c, suggesting that only a portion of binding sites was occupied. In contrast, the peak current of the NIPs/MWCNTs/GCE after removal (Fig. 4B, curve b) was only a little higher than that of the electrode before removal (Fig. 4B, curve a), and the immersion in the HIV-p24 solution induced quite a small change in current (Fig. 4B, curve c) compared to the MIPs/MWCNTs/GCE due to the no imprinted cavities in the NIPs, which was prepared in the absence of HIV-p24. Fig. 4C shows the DPV of electrode without MWCNTs modified before removal of HIV-p24 from polymer (curve a), after removal of HIV-p24 from polymer (curve b) and after incubating in 0.01 ng cm^{-3} HIV-p24 solution for 10 min (curve c), a similar trend has been obtained, but without MWCNTs, the GCEs show very low peak of current, which proved MWCNTs accelerate the electron transfer and increase the specific surface area once again.

3.3. Calibration curve for electrochemical determination of HIV-p24

Fig. 5 demonstrated the DPV curves of the re-adsorption of MIPs/MWCNTs/GCE with different HIV-p24 concentrations. As shown in Fig. 5A, the DPV peak current of the MIPs/MWCNTs/GCE decreased with the increasing HIV-p24 concentrations ascribed to the rebinding of HIV-p24 to the imprinting sites. The relationship between currents (i) and the concentrations of HIV-p24 was exhibited in Fig. 5B. It can be seen that the calibration curve for the determination of HIV-p24 is composed of two distinct straight lines, suggesting that there are two types of binding sites, which named as high affinity binding sites and low affinity binding sites [31], existed in the HIV-p24-imprinted polymer. The linear regression equations for the HIV-p24 concentrations ranged from 1.0×10^{-4} to 0.01 ng cm^{-3} and 0.01–2 ng cm^{-3} are obtained as i=−3608.95c (ng cm^{-3}) +201.18 (r^2=0.995) and i=−27.87c (ng cm^{-3})+165.79 (r^2=0.997), respectively. The limit of detection (LOD, S/N=3) of the sensor, which is defined as the lowest concentration of HIV-p24 could be found was low to 0.083 pg cm^{-3}. LOD was determined by the following equations, where LOD=3 S/K $S=\sqrt{\frac{\sum_{i=1}^{n}(X_i-\overline{X})}{n-1}}\overline{X}=\frac{X_1+X_2\cdots+X_n}{n}$ n is the number of the measurement of the blank sample, now it is the measurement times of the MIPs/MWCNTs/GCE after the removal of HIV-p24. K is the slope of linear response equations. The reasons for this might be up to two factors:

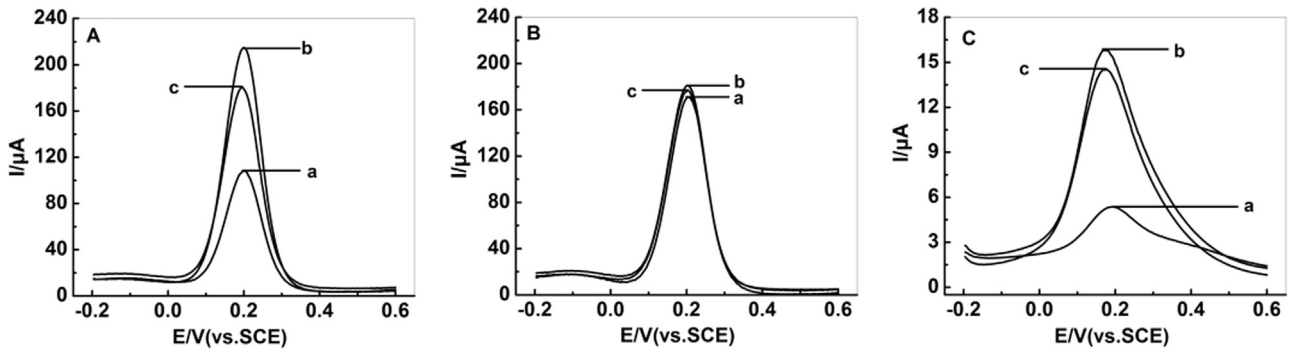

Fig. 4. The DPV curves of MIPs/MWCNTs/GCE (A), NIPs/MWCNTs/GCE (B) and MIPs/GCE (C) in PBS (pH 7.0) containing 10 mmol dm^{-3} $[Fe(CN)_6]^{3-/4-}$ and 0.1 mol dm^{-3} KCl: (a) before removal of HIV-p24 from polymer; (b) after removal of HIV-p24 from polymer; (c) after incubating in 0.01 ng cm^{-3} HIV-p24 solution for 10 min.

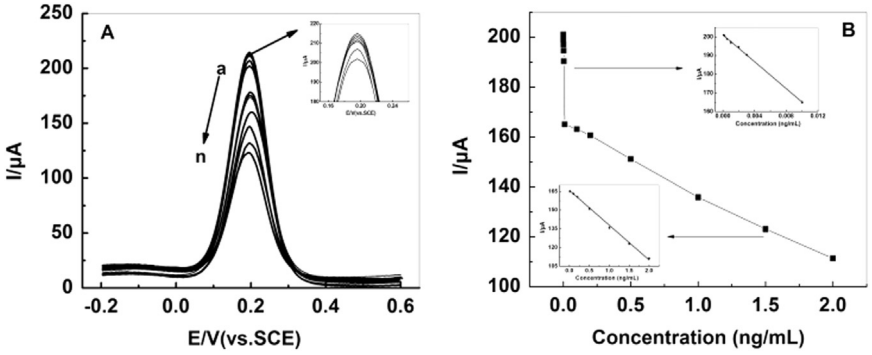

Fig. 5. The DPV curves of MIP/MWCNTs/GCE electrode in PBS (pH 7.0) containing 10 mmol dm^{-3} $[Fe(CN)_6]^{3-/4-}$ and 0.1 mol dm^{-3} KCl after rebinding with HIV-p24 (concentration of HIV-p24 from curve a to curve n were 0, 1.0×10^{-4}, 2×10^{-4}, 5×10^{-4}, 10^{-3}, 2×10^{-3}, 3×10^{-3}, 0.01, 0.1, 0.2, 0.5, 1, 1.5 and 2 ng cm^{-3}) (A). The calibration plot of MIPs/MWCNTs/GCE electrode (B).

Firstly, the excellent electrical conductivity of MWCNTs enhanced the charge transfer; secondly, the formation of CS film increased the immobilization amount of HIV-p24 by the GA cross-linker. Table 1 presents a detailed comparison of the performance of different systems towards the determination of HIV-p24. In contrast with the previously reported methods, the MWCNTs based MIP electrochemical sensor for the determination of HIV-p24 showed a wider linear range with a lower detection limits.

3.4. Selectivity of the MIPs sensor

To evaluate the selectivity of the HIV-p24 (24 kDa) imprinted polymer, we chose some structurally similar as well as coexistent species in serum with HIV-p24, such as CEA (180 kDa), HCG (36 kDa), AFP (66 kDa) and BSA (MW 66 kDa) as potential interferents for comparison experiments. DPV responses of the proposed MIPs/MWCNTs/GCE in a 0.01 ng cm^{-3} HIV-p24 solution with or without different interference (0.01 ng cm^{-3}) were assayed. The signal responses (ΔI) of $[Fe(CN)_6]^{3-/4-}$ on the MIPs/MWCNTs/GCE and the NIPs/MWCNTs/GCE after incubating of each interference were shown in Fig. 6. The ΔI value of the MIPs/MWCNTs/GCE electrode toward HIV-p24 was 35.9 μA, which was 23.25, 32.98, 30.69 and 27.71 times higher than that towards CEA, HCG, AFP and BSA, respectively. The results indicates that the proposed MIPs/MWCNTs/GCE biosensor favors HIV-p24 and has good selectivity toward the target protein.

The selectivity was further evaluated by imprinting factor β, which was calculated as following: $\beta=\Delta I_{MIPs/MWCNTs/GCE}/\Delta I_{NIPs/MWCNTs/GCE}$. The β values were 19.73, 3.67, 3.4, 4.33 and 3.02 for HIV-p24 CEA, HCG, AFP and BSA, respectively. The β value for HIV-p24 suggested that MIPs/MWCNTs/GCE possessed a much higher capacity toward HIV-p24 than NIPs/MWCNTs/GCE electrode. It also provides a direct evidence for the good selectivity of MIPs/MWCNTs/ GCE.

Table 1
Comparison of performances of the MWCNTs based MIPs electrochemical sensor with other immunoassay systems.

Materials	Linear range (ng cm^{-3})	Limit of detection (pg cm^{-3})	Reference
Mercapto succinic acid hydrazide copper monolayer	0.5~200	200	[32]
DNA modified gold nanoparticles	2.4×10^{-3} ~ 2.4	7.9×10^{-8}	[33]
Goldnanoparticles/CNTs/ acetone-extracted propolis nanocomposite	0.01~60	6.4	[34]
Electroplating-gold electrode	0.01–100	8	[35]
Fe_3O_4@SiO_2 nanomagnetic	0.001–10	0.5	[36]
Europium nanoparticle-based microtiter-plate immunoassay	0~0.5	3.7	[37]
Graphene oxide-carbon nanotubes-silica electrode	5.0×10^{-4}~8.5	0.15	[38]
SERS-based lateral flow assay biosensor	0.008 ~ 64	0.24	[39]
MWCNTs based MIP electrochemical sensor	1.0×10^{-4} ~2	0.083	This work

3.5. Repeatability, reproducibility and stability

Repeatability, reproducibility and stability are key parameters to evaluate the applicability of electrochemical sensor. The MIPs/MWCNTs/GCE sensor preserved their repeatability by successively applying a sensor to a 0.01 ng cm^{-3} of HIV-p24 for five times. No significant changes on the DPV signals were observed. The relative standard deviation (RSD) was obtained as 1.03%, indicating that the MIPs/MWCNTs/GCE sensor had a good repeatability. We also prepared five MIPs/MWCNTs/GCE sensors under the same conditions to evaluate the reproducibility in the HIV-p24 solution. The RSD of peak current is 1.21%, implying excellent reproducibility. The stability of the MIPs/MWCNTs/GCE sensor towards 0.01 ng cm^{-3} HIV-p24 was also examined periodically. After stored in a refrigerator at 4 °C for 5 days, the redox current obtained from the as-prepared electrode remained almost the same. When the electrode was stored for 10 days under the same condition, the peak current was still retained 98.57% of its initial value, indicating that the developed sensor possesses high stability.

3.6. Applications in real samples

In order to investigate the practical applications of the proposed method for the determination of HIV-p24, the MIPs/MWCNTs/GCE

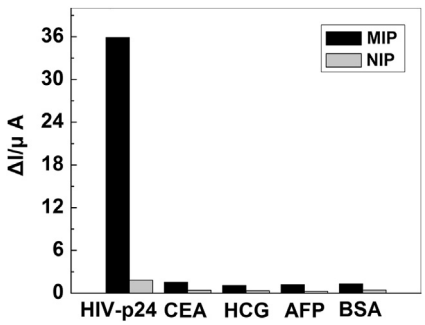

Fig. 6. The current responses of the MIPs/MWCNTs/GCE and NIPs/MWCNTs/GCE electrode after rebinding with HIV-p24, CEA, HCG, AFP, and BSA.

Table 2A
Recoveries of HIV-p24 determination in human serum sample.

Sample	The amount of HIV-p24 added (ng cm^{-3})	The amount of HIV-p24 detected (ng cm^{-3})	Recovery (%)	RSD (%) (n=3)
1	0.03	0.0301	100.3	1.1
2	0.05	0.0502	100.4	1.3
3	0.1	0.0982	98.20	1.8
4	0.5	0.512	102.4	2.5
5	1.5	1.49	99.33	2.1

Table 2B
Determination of HIV-p24 in human serum samples.

Sample	Proposed MIPs sensor (ng cm^{-3}, n=6)	The reference method (ELISA) (ng cm^{-3})	Relative deviation (%)
1	0.0022	0.0021	−4.7
2	0.0063	0.0061	3.3
3	0.031	0.029	3.4
4	0.063	0.062	−1.7
5	0.42	0.41	−1.2
6	0.63	0.61	1.1
7	0.92	0.91	1.2
8	1.5	1.5	2.1
9	1.8	1.79	−0.11
10	2.0	2.1	1.3

sensor was applied to assay different concentrations of HIV-p24 in human serum by a standard addition method. As shown in Table 2A, the average recovery of one sensor which measured three times was in the range of 98.20–102.4% and RSD of the three values for one sensor was under the scope of 1.1–2.5% in all test samples, demonstrating good precision and accuracy nature. To further investigate the practical application of the MIPs-based sensor, we got ten human serum specimens from Military Region General Hospital of Guangzhou, and evaluated by using the developed method and the reference ELISA method, respectively. The results are listed in Table 2B, it can be seen that the relative errors between the two methods ranged from −4.7–3.4%, which indicates that there is no significant difference between the results given by the two methods, that is, the developed MIPs-based method could be potentially used for determination of HIV-p24 in biological samples and provides an interesting tool for detection protein in clinical laboratory.

4. Conclusions

A novel surface molecular imprinting strategy for rapid, convenient and sensitive detection of HIV-p24 through imprinting HIV-p24 template molecules on the surface of MWCNTs modified electrode was proposed in the present work. The purpose of introduction of MWCNTs is to use its specific surface area, excellent electrocatalytic performance and remarkable electrical conductivity to improve the detection sensitivity of the sensor. The established method has been validated to be reliable, highly sensitive and selective, and the LOD for HIV-p24 was pushed to 0.083 pg cm^{-3}, which was remarkably lower than other current techniques. The method described here opens a new approach for simple, low cost, effective and sensitive determination of HIV-p24 antigen, and provide a promising potential in clinical applications.

Acknowledgements

This work was financially supported by the National Natural Science Foundation of China (Grant Nos. 21475046, 21427809). We also acknowledge the Fundamental Research Funds for the Central Universities (No. 2015ZM050 and 2015ZP028).

References

[1] D. Nadal, J. Boni, C. Kind, O.E. Varnier, F. Steiner, Z. Tomasik, J. Schupbach, Prospective evaluation of amplification-boosted ELISA for heat-denatured p24 antigen for diagnosis and monitoring of pediatric human immunodeficiency virus type 1 infection, J. Infect. Dis. 180 (1999) 1089–1095.
[2] L. Zheng, L.Y. Jia, B. Li, B. Situ, Q.L. Liu, Q. Wang, N. Gan, A sandwich HIV p24 amperometric immunosensor based on a direct gold electroplating-modified electrode, Molecules 17 (2012) 5988–6000.
[3] A. Biancotto, B. Brichacek, S.S. Chen, W. Fitzgerald, A. Lisco, C. Vanpouille, L. Margolis, J.C. Grivel, A highly sensitive and dynamic immunofluorescent cytometric bead assay for the detection of HIV-1 p24, J. Virol. Methods 157 (2009) 98–101.
[4] D.M. Perez-Filgueir, B.P. Brayfield, S. Phiri, M.V. Borca, C. Wood, T.J. Morris, Preserved antigenicity of HIV-1 p24 produced and purified in high yields from plants inoculated with a tobacco mosaic virus (TMV)-derived vector, J. Virol. Methods 121 (2004) 201–208.
[5] V.C. Priscila, T.C. Patricia, F.G. Assuero, M.B.A. Leila, U.A. Paula, Heterologous expression, characterization and structural studies of a hydrophobic peptide from the HIV-1 p24 protein, Peptides 26 (2005) 243–249.
[6] T.A. Tshishi, S.M. Ditu, B.M. Kabwe, M.K. Philomène, S.B. Anaclet, A sensitive radioimmunoassay of human immunodeficiency virus type-1 p24 antigen in serum, Immuno-anal, Biol. Spéc. 22 (2007) 190–193.
[7] R. Kannangai, S. Ramalingam, K.J. Prakash, O.C. Abraham, R. George, R.C. Castillo, D.H. Schwartz, M.V. Jesudason, G. Sridharan, A peptide enzyme linked immunosorbent assay (ELISA) for the detection of human immunodeficiency virus type-2 (HIV-2) antibodies: an evaluation on polymerase chain reaction (PCR) confirmed samples, J. Clin. Virol. 22 (2001) 41–46.
[8] R. Sutthent, N. Gaudart, K. Chokpaibulkit, N. Tanliang, C. Kanoksinsombath, P. Chaisilwatana, p24 antigen detection assay modified with a booster step for diagnosis and monitoring of human immunodeficiency virus type 1 infection, J. Clin. Microbiol. 41 (2003) 1016–1022.
[9] F. Akhgari, H. Fattahi, Y.M. Oskoei, Recent advances in nanomaterial-based sensors for detection of trace nitroaromatic explosives, Sens. Actuators B 221 (2015) 867–878.
[10] L.X. Chen, X.Y. Wang, W.H. Lu, X.Q. Wu, J.H. Li, Molecular imprinting: perspectives and applications, Chem. Soc. Rev. 45 (2016) 2137–2211.
[11] L.X. Chen, Sh.F. Xu, J.H. Li, Recent advances in molecular imprinting technology: current status, challenges and highlighted applications, Chem. Soc. Rev. 40 (2011) 2922–2942.
[12] S. Tokonami, H. Shiigi, T. Nagaoka, Review: micro- and nanosized molecularly imprinted polymers for high-throughput analytical applications, Anal. Chim. Acta 641 (2009) 7–13.
[13] X.R. Xing, S. Liu, J.H. Yu, W.J. Lian, J.D. Huang, Electrochemical sensor based on molecularly imprinted film at polypyrrole-sulfonated graphene/hyaluronic acid-multiwalled carbon nanotubes modified electrode for determination of tryptamine, Biosens. Bioelectron. 31 (2012) 277–283.
[14] J.A. García-Calzón, M.E. Díaz-García, Characterization of binding sites in molecularly imprinted polymers, Sens. Actuators B 123 (2007) 1180–1194.
[15] J.P. Li, Y.J. Shao, W.L. Yin, Y. Zhang, A strategy for improving the sensitivity of molecularly imprinted electrochemical sensors based on catalytic copper deposition, Anal. Chim. Acta 817 (2014) 17–22.
[16] B. Liu, H.T. Lian, J.F. Yin, X.Y. Sun, Dopamine molecularly imprinted electrochemical sensor based on graphene-chitosan composite, Electrochim. Acta 75 (2012) 108–114.
[17] J.P. Li, W.L. Yin, Y.J. Tan, H.C. Pan, A sensitive electrochemical molecularly imprinted sensor based on catalytic amplification by silver nanoparticles for 3-indoleacetic acid determination, Sens. Actuators B 197 (2014) 109–115.
[18] Y.K. Yang, G.Z. Fang, G.Y. Liu, M.F. Pan, X.M. Wang, L.J. Kong, X.L. He, S. Wang, Electrochemical sensor based on molecularly imprinted polymer film via sol-gel technology and multi-walled carbon nanotubes-chitosan functional layer for sensitive determination of quinoxaline-2-carboxylic acid, Biosens. Bioelectron. 47 (2013) 475–481.
[19] F.T.C. Moreira, R.A.F. Dutra, J.P.C. Noronha, J.C.S. Fernandes, M.G.F. Sales, Novel biosensing device for point-of-care applications with plastic antibodies grown on Au-screen printed electrodes, Sens. Actuators B 182 (2013) 733–740.
[20] Y. Sun, H.Y. Du, Y.T. Lan, W.J. Wang, Y.J. Liang, Ch.L. Feng, M. Yang, Preparation of hemoglobin (Hb) imprinted polymer by Hb catalyzed eATRP and its application in biosensor, Biosens. Bioelectron. 77 (2016) 894–900.
[21] K. Haupt, K. Mosbach, Molecularly imprinted polymers and their use in biomimetic sensors, Chem. Rev. 100 (2000) 2495–2504.
[22] Y. Liang, L. Gu, X.Q. Liu, Q.Y. Yang, H. Kajiura, Y.M. Li, T. Sh Zhou, G.Y. Shi, Composites of polyaniline nanofibers and molecularly imprinted polymers for recognition of nitroaromatic compounds, Chemistry 17 (2011) 5989–5997.
[23] Y.B. Zeng, Y. Zhou, L. Kong, T.S. Zhou, G.Y. Shi, A novel composite of SiO_2-coated graphene oxide and molecularly imprinted polymers for electrochemical sensing dopamine, Biosens. Bioelectron. 45 (2013) 25–33.
[24] H. Wang, W. Zhou, X. Yin, Z. Zhuang, H. Yang, X.R. Wang, Template synthesized molecularly imprinted polymer nanotube membranes for chemical separations, J. Am. Chem. Soc. 128 (2006) 15954–15955.
[25] X.W. Kan, Y. Zhao, Z.R. Geng, Z.L. Wang, J.J. Zhu, Composites of multi-walled

carbon nanotubes and molecularly imprinted polymers for dopamine recognition, J. Phys. Chem. C. 112 (2008) 4849–4854.
[26] J. Tkac, J.W. Whittaker, T. Ruzgas, The use of single walled carbon nanotubes dispersed in a chitosan matrix for preparation of a galactose biosensor, Biosens. Bioelectron. 22 (2007) 1820–1824.
[27] M.W. Shen, S.H. Wang, X.Y. Shi, X.S. Chen, Q.G. Huang, E.J. Petersen, R.A. Pinto, J.R. Baker Jr., W.J. Weber Jr., Polyethyleneimine-mediated functionalization of multiwalled carbon nanotubes: synthesis, characterization, and in vitro toxicity assay, J. Phys. Chem. C. 113 (2009) 3150–3156.
[28] G.S. Lai, F. Yan, J. Wu, Ch Leng, H.X. Ju, Ultrasensitive multiplexed immunoassay with electrochemical stripping analysis of silver nanoparticles catalytically deposited by gold nanoparticles and enzymatic reaction, Anal. Chem. 83 (2011) 2726–2732.
[29] R.P. Liang, Zh.X. Wang, Li Zhang, J.D. Qiu, A label-free amperometric immunosensor for alpha-fetoprotein determination based on highly ordered porous multiwalled carbon nanotubes/silica nanoparticles array platform, Sens. Actuators B 166–167 (2012) 569–575.
[30] A. Fatoni, A. Numnuam, P. Kanatharana, W. Limbut, P. Thavarungkul, A novel molecularly imprinted chitosan-acrylamide, graphene, ferrocene composite cryogel biosensor used to detect microalbumin, Analyst 139 (2014) 6160–6167.
[31] H.P. Bai, Ch.Q. Wang, J. Chen, J. Peng, Q. Cao, A novel sensitive electrochemical sensor based on in-situ polymerized molecularly imprinted membranes at graphene modified electrode for artemisinin determination, Biosens. Bioelectron. 64 (2015) 352–358.
[32] N. Gan, T.H. Li, J.P. Lei, L.Y. Wang, X. Yang, Electrochemical immunosensor for human immunodeficiency virus p24 antigen based on mercapto succinic acid hydrazide copper monolayer modified gold electrode, Chin. J. Anal. Chem. 36 (2008) 1167–1171.
[33] K. Teeparuksapun, M. Hedstrom, E.Y. Wong, S. Tang, I.K. Hewlett, B. Mattiasson, Ultrasensitive detection of HIV-1 p24 antigen using nanofunctionalized surfaces in a capacitive immunosensor, Anal. Chem. 82 (2010) 8406–8411.
[34] F. Kheiri, R.E. Sabzi, E. Jannatdoust, E. Shojaeefar, H. Sedghi, A novel amperometric immunosensor based on acetone-extracted propolis for the detection of the HIV-1 p24 antigen, Biosens. Bioelectron. 26 (2011) 4457–4463.
[35] L. Zheng, L.Y. Jia, B. Li, B. Situ, Q.L. Liu, Q. Wang, N. Gan, A sandwich HIV p24 amperometric immunosensor based on a direct gold electroplating-modified electrode, Molecules 17 (2012) 5988–6000.
[36] N. Gan, X.W. Du, Y.T. Cao, F.T. Hu, T.H. Li, Q.L. Jiang, An ultrasensitive electrochemical immunosensor for HIV p24 based on Fe_3O_4@SiO_2 nanomagnetic probes and nanogold colloid-labeled enzyme-antibody copolymer as signal tag, Materials 6 (2013) 1255–1269.
[37] J.K. Liu, B. Ch Du, P.H. Zhang, M.H. Haleyurgirisetty, J.Q. Zhao, V. Ragupathy, S. Lee, D.L. DeVoe, I.K. Hewlett, Development of a microchip Europium nanoparticle immunoassay for sensitive point-of-care HIV detection, Biosens. Bioelectron. 61 (2014) 177–183.
[38] Y.S. Fang, X.J. Huang, L. Sh Wang, J.F. Wang, An enhanced sensitive electrochemical immunosensor based on efficient encapsulation of enzyme in silica matrix for the detection of human immunodeficiency virus p24, Biosens. Bioelectron. 64 (2015) 324–332.
[39] X.L. Fu, Z.Y. Cheng, J.M. Yu, P. Choo, L.X. Chen, J. Choo, A SERS-based lateral flow assay biosensor for highly sensitive detection of HIV-1 DNA, Biosens. Bioelectron. 78 (2016) 530–537.